Pharm Res (2010) 27:2433–2445
DOI 10.1007/s11095-010-0236-1

RESEARCH PAPER

Reliability of Inhibition Models to Correctly Identify Type of Inhibition

Vidula Kolhatkar • James E. Polli

Received: 3 June 2010 / Accepted: 2 August 2010 / Published online: 14 August 2010

ABSTRACT

Purpose Type of inhibition (e.g. competitive, noncompetitive) is frequently evaluated to understand transporter structure/function relationships, but reliability of nonlinear regression to correctly identify inhibition type has not been assessed. The purpose was to assess the ability of nonlinear regression to correctly identify inhibition type.

Methods This aim was pursued through three objectives that compared the competitive, noncompetitive, and uncompetitive inhibition models to best fit simulated competitive and noncompetitive data. The first objective involved conventional inhibition data and entailed simulated data for the common situation where substrate concentration was fixed at a single level but inhibitor concentration varied. The second objective involved Dixon-type data where both substrate and inhibitor concentrations varied. A third objective involved nonconventional inhibition data, where substrate concentration was varied and inhibitor was fixed at a single concentration. Experimental data were also examined.

Results Nonlinear regression performed poorly in identifying the correct inhibition model for conventional inhibition data, but performed moderately well for Dixon-type data. Interestingly, nonlinear regression performed well for nonconventional inhibition data, particularly at higher inhibitor concentrations. Experimental data support simulation findings.

Conclusions Conventional inhibition data is a poor basis to determine inhibition type, while Dixon-type data affords modest success. Nonconventional inhibition data merits further consideration.

KEY WORDS competitive inhibition · dixon plot · model · noncompetitive inhibition · transporter

INTRODUCTION

Inhibition studies are routinely performed to gain insight into the structure and function of transporters, particularly when a transporter crystal structure is not available. For example, two project areas in our laboratory involve the apical sodium-dependent bile acid transporter (ASBT) and the organic cation/carnitine transporter (OCTN2), where transport inhibition studies by novel compounds and diverse drugs have yielded pharmacophore models and quantitative structure-activity relationships (QSAR) (1–4). A simplifying assumption in proposing such pharmacophore or QSAR models is that inhibition data assumes the same type of inhibition, since two compounds that inhibit a transporter by differing mode may not bind to the same binding site. Hence, inhibition studies can benefit from elucidating the type of inhibition by which various compounds inhibit. Determining type of inhibition can also help in understanding of interaction of inhibitors at the binding site of transporter. For example, enalapril was concluded to be a competitive inhibitor of glycylsarcosine transport by the high-affinity peptide transporter (5), whereas quinapril was concluded to be a noncompetitive inhibitor (6). These conclusions suggested that enalapril and glycylsarcosine bind at the same binding site, whereas quinapril binds at a different binding site than glycylsarcosine. Thus, determining type of inhibition contributes towards transporter structure/function understanding.

Electronic supplementary material The online version of this article (doi:10.1007/s11095-010-0236-1) contains supplementary material, which is available to authorized users.

V. Kolhatkar • J. E. Polli (✉)
University of Maryland School of Pharmacy
20 Penn Street, HSF2 Room 623
Baltimore, Maryland 21201, USA
e-mail: jpolli@rx.umaryland.edu

Classic inhibition models include competitive, noncompetitive, and uncompetitive inhibition. Although these models have long-standing use, it has not been assessed when the competitive and noncompetitive models are reliable in correctly elucidating the type of inhibition. One common approach to discern between competitive and noncompetitive inhibition is via nonlinear regression and selection of the better fitting model. For instance, Lau and Chang studied CYP2B6 inhibition by *Ginkgo biloba* extract (7). Mode of inhibition was determined through inhibition studies that used various inhibitor and substrate concentrations, followed by nonlinear regression for competitive, noncompetitive, mixed and uncompetitive inhibition. The result was verified by visual inspection of a Lineweaver-Burk plot and a Dixon plot. However, reliability of methods to identify the correct model has not been evaluated in such applications. The other approach to discern between types of inhibition involves measuring changes in substrate parameters Kt and Jmax with change in inhibitor concentration.

Three objectives were pursued that concerned the ability to correctly identify the correct type of inhibition. The first objective was to compare the abilities of the competitive, noncompetitive, and uncompetitive inhibition models to best fit simulated competitive and noncompetitive data, where data reflected conventional inhibition data. Conventional inhibition data entailed simulated data for the common situation where substrate concentration was fixed at a single level but inhibitor concentration varied. The second objective was identical to this first objective, but considered so-called Dixon-type data, where simulated data was larger in scope, in that both substrate concentration and inhibitor concentration were varied. These objectives were pursued by simulating uptake values for each competitive and noncompetitive inhibition model using an Excel spreadsheet; Gaussian error was then incorporated to the uptake values. These simulated data were subjected to nonlinear model fitting, and the best fitting model was identified. Since results showed that nonlinear regression performed poorly in identifying the correct inhibition model for conventional inhibition data, a third objective was pursued, which was to perform similar studies as per the first objective but for nonconventional inhibition data, where substrate concentration was varied and inhibitor concentration was fixed at a single level. Results from experimental inhibition data were also examined to challenge simulation observations.

Overall findings here suggest caution in suggesting a specific inhibition model from various types of inhibition data, including conventional data and even the more comprehensive Dixon-type data. Additionally, results indicate that nonconventional inhibition data merits further consideration to identify type of inhibition, particularly since such an approach is resource sparing compared to Dixon-type data.

MATERIALS AND METHODS

To assess the ability to correctly identify type of inhibition, three objectives were pursued using simulated uptake data, where each objective differed in scope of data. The first objective employed simulated uptake where substrate concentration was fixed at a single level but inhibitor concentration varied (conventional inhibition data). The second objective employed simulated uptake where both substrate and inhibitor concentrations were varied (Dixon-type data). The third objective employed simulated uptake where substrate concentration was varied but inhibitor concentration was fixed at a single level (nonconventional inhibition data). These objectives involved data simulation, followed by model fitting and comparison of model performance. Simulations were employed since only simulation can provide a basis to know with certainty the underlying inhibition type. Results from experimental inhibition data were also examined to challenge the observations from simulation studies.

Analysis of Conventional Inhibition Data

Data Simulation

Simulated uptake values were obtained from competitive and noncompetitive inhibition models. The competitive and noncompetitive inhibition models are shown in Eqs. 1 and 2.

$$\mathcal{J} = \frac{\mathcal{J}_{\max} S}{K_t(1 + I/K_i) + S} \tag{1}$$

$$\mathcal{J} = \frac{\mathcal{J}_{\max} S}{(1 + I/K_i)(K_t + S)} \tag{2}$$

where $\mathcal{J}$ is solute uptake, S is solute concentration, $\mathcal{J}$max and Kt are the Michaelis-Menten constants for transporter-mediated uptake of solute, Ki is the inhibition coefficient, and I is inhibitor concentration. Passive flux was considered zero for simplicity. Simulations were performed with the following parameters: $\mathcal{J}$max = 0.0005 nmol/s/cm^2; Kt = 5 μM; S = 2.5 μM. Three scenarios were studied. In the first scenario, simulated uptake values were obtained from the competitive model where Ki was 10 μM and inhibitor concentration varied from 0 to 100 μM. In the second scenario, simulated uptake values were obtained from each competitive and noncompetitive model where Ki was 100 μM and inhibitor concentration varied from 0 to 500 μM, as well as from 0 to 1,000 μM. These values for Ki, I, Kt, and S were assessed since these values reflect typical ranges in the literature. Simulated uptake values

were not obtained from the uncompetitive inhibition model, since this model is of less general interest than the other two models.

Uptake error was computed using Excel. Error in uptake was incorporated using a percent coefficient of variation (CV%) level of 30% and 10%, which reflects a higher and lower end of common level of variation. Error was added by multiplying the simulated uptake value from Eqs. 1 or 2 by a random number with mean 1.0 and standard deviation 0.3 or 0.1. Profiles were simulated to allow for each scenario to be evaluated 30 times (i.e. 30 occasions), which is a large sample size (8). For each occasion, simulations attempted to mimic experimental design using $n=3$, such that each uptake value was simulated (with error) three times for each unique condition for each occasion.

Model Fitting and Identification of Best Fitting Model

The competitive, noncompetitive, and uncompetitive inhibition models were fitted to the simulated data using WinNonlin 5.2 (Pharsight, Mountain View, CA). The competitive and noncompetitive models are Eqs. 1 and 2, respectively. The uncompetitive model is

$$\mathcal{J} = \frac{\mathcal{J}_{\max} S}{K_t + S(1 + I/K_i)} \tag{3}$$

Akaike Information Criterion (AIC) was used to select the best fitting model from the competing models (9).

$$AIC = n \cdot \ln\left(\sum_{i=1}^{n} w_i \left(\Upsilon_{obs,i} - \Upsilon_{cal,i}\right)^2\right) + 2p \tag{4}$$

where n is the number of data points, i is the sequence sample number, wi is the weight (wi = 1), $\Upsilon obs,i$ is the observed value, $\Upsilon cal,i$ is the predicted value, and p is the number of model parameters.

Ki estimates from the correct model (even if not the best fitting model) were evaluated in terms of accuracy by comparing the Ki estimate to the true Ki (i.e. Ki value used to simulate the data).

Analysis of Dixon-Type Data

Data Simulation

Simulated uptake values with error were obtained from competitive and noncompetitive inhibition models as above, using Eqs. 1 and 2. Simulations for two scenarios were conducted to mimic a matrix of inhibition studies involving three levels of substrate concentration, as well as four levels of inhibitor concentrations (i.e. conducted to mimic the large scope of data that is historically analyzed by Dixon plots). In the first simulation scenario, which covers a wide range of I/Ki, the following parameter ranges were used: $\mathcal{J}$max was 0.0005 nmol/s/cm^2; S was 1, 5, and 10 μM; when Ki was 1 μM, I = 0, 0.5, 2 and 5 μM; and when Ki = 100 μM, I = 0, 50, 200, and 500 μM. The ratio I/Ki ranged from 0 to 5.

The following parameter ranges were used in a second simulation scenario with a more narrow, but more experimentally-typical range, of I/Ki values: $\mathcal{J}$max was 0.0002 nmol/s/cm^2; Kt was 5 μM; S was 1, 2.5, and 5 μM; Ki = 58 μM; and I was 0, 10, 50, and 100 μM. The ratio I/Ki ranged from 0 to 1.7, which reflects the typical range of I/Ki values (10–15).

Error was incorporated using a CV% level of 20% or 30%, as described above. Uptake profiles were simulated to allow for each scenario to be evaluated 30 times (i.e. 30 occasions), which is a large sample size (8). For each occasion, simulations attempted to mimic experimental design using $n=3$, such that each uptake value was simulated (with error) three times for each unique condition for each occasion.

Model Fitting and Identification of Best Fitting Model

As above for the first objective, primary analysis of this Dixon-type data was non-linear regression, and not Dixon plot analysis. For each the competitive, noncompetitive and uncompetitive inhibition models, fits of Eqs. 1, 2, and 3 to simulated data were conducted using WinNonlin. Simultaneous fitting of uptake *versus* inhibitor concentration was conducted across the three levels of substrate concentration. AIC was used in selecting the best fitting model. Ki estimates from the best fitting nonlinear regression model were also examined in terms of accuracy, by comparing to the Ki value used to simulate the data. As secondary analysis to nonlinear regression, simulated uptake data were plotted as Dixon plots; plots were visually assessed to determine type of inhibition.

Analysis of Nonconventional Inhibition Data

As results below indicate, conventional inhibition data performed poorly in identifying the correct inhibition model. Additionally, Dixon-type data requires a large and comprehensive matrix of inhibition studies, which represents a practical barrier to routinely elucidate type of inhibition. Hence, nonconventional inhibition data—where substrate concentration was varied but inhibitor concentration was fixed at a single level—were assessed for its ability to identify the correct inhibition model, even though such studies are generally not performed. Of note, data for this third objective was practically the same as for the first

objective (i.e. same simulation approach and same range of parameter values); first and third objectives only differed in data groupings that were subjected to model regression, although were simulated separately.

Data Simulation

Simulated uptake values with error were obtained from competitive and noncompetitive inhibition models as above, using Eqs. 1 and 2. Simulations were conducted over following parameter ranges: $\mathcal{J}$max=0.0005 nmol/s/cm^2; Ki=5 μM (as well as 500 μM for competitive model); S ranged from 0.2 times Ki to 100 times Ki; and I/Ki ranged from 0.01 to 100.

Model Fitting and Identification of Best Fitting Model

The competitive, noncompetitive and uncompetitive inhibition models were fit to the simulated data using WinNonlin 5.2. AIC was used in selecting the best fitting model from the competing models.

Experimental Data

Materials

Ursodeoxycholic acid was purchased from TCI America (Portland, OR, USA), taurocholic acid was purchased from Calbiochem (La Jolla, CA, USA) and (^{3}H) taurocholic acid was obtained from PerkinElmer (Waltham, MA, USA).

Inhibition Studies

Inhibition studies were performed in hASBT-MDCK cell line as described previously (3). Briefly, the cells were exposed to donor solution containing taurocholate (spiked with ^{3}H taurocholate), and the inhibitor at 37°C for 10 min. After 10 min, cells were lysed, and cell lysate was counted for associated radioactivity using a liquid scintillation counter.

Conventional inhibition data were obtained via an inhibition study using one fixed level of substrate concentration (i.e. 2.5 μM taurocholic acid). Ursodeoxycholic acid was used as inhibitor; inhibitor concentration ranged from 0 to 250 μM. Dixon-type data was obtained via an inhibition study using three taurocholate substrate concentrations (1, 2.5 and 5 μM) and four ursodeoxycholate concentrations (0, 25, 50 and 100 μM). Nonconventional inhibition data was obtained via an inhibition study performed at several taurocholate substrate concentrations ranging from 1 to 500 μM and one inhibitor (ursodeoxycholate) concentration. Two sets of nonconventional inhibition data were obtained: one at I/Ki=1 and the other at I/Ki=5.

Similar to Eqs. 1–3, inhibition data were fitted to the competitive, noncompetitive, and uncompetitive models, but allowed for a passive permeability component, per Eqs. 5–7:

$$\mathcal{J} = \frac{\mathcal{J}_{\max} S}{K_t(1 + I/K_i) + S} + P_p S \tag{5}$$

$$\mathcal{J} = \frac{\mathcal{J}_{\max} S}{(1 + I/K_i)(K_t + S)} + P_p S \tag{6}$$

$$\mathcal{J} = \frac{\mathcal{J}_{\max} S}{K_t + S(1 + I/K_i)} + P_p S \tag{7}$$

where Pp is the passive permeability.

RESULTS AND DISCUSSION

Analysis of Conventional Inhibition Data

Simulated Competitive Model Data

The first objective was to compare the abilities of competitive, noncompetitive, and uncompetitive inhibition models to best fit simulated competitive and noncompetitive data from conventional inhibition studies. Tables I and II summarize results obtained from simulated competitive data and simulated noncompetitive data, respectively.

In Table I, study variables were model used to fit data (competitive, noncompetitive, and uncompetitive), Ki (10 and 100 μM), maximum I/Ki ratio (5 and 10), and error level (%CV of 10% and 30%). When Ki=10 μM, maximum I/Ki=10, and error is 30%, the competitive model (i.e. the correct model) was the best fitting model only 36.7% of the time. The uncompetitive mode was the best fitting 46.7% of the time.

Fig. 1 plots the simulated conventional inhibition data for two occasions (one occasion in panel A and another occasion in panel B). These data reflect conventional inhibition data, where uptake from a fixed, single concentration of substrate is reduced as inhibitor concentration is increased. Fig. 1 shows the fits of all three models to simulated competitive data when Ki=10 μM. In Fig. 1 panel A, the uncompetitive model was the best fitting model, where r^2 was 0.900 for competitive, noncompetitive and uncompetitive fits. All three fit profiles were practically the same. For this simulation occasion (of the total of 30 independent occasions), AIC values did not determine the competitive model to be the best fitting model. Meanwhile, in panel B, the competitive model was the best fitting model

Table I Results from Conventional Inhibition Data. Data were Simulated from Competitive Inhibition Model, where Ki, Maximum I/Ki, and Random Error were Varied. Under Best Fitting Model, Values are the Percentage of Times that the Best Fitting Model was Competitive, Noncompetitive, or Uncompetitive. Percentages are Derived from Simulations of 30 Occasions ($n=3$ Per Occasion). AIC was Used to Identify the Best Fitting Model

Ki (μM)	Maximum I/Ki	%CV error	Best fitting model		
			Competitive	Noncompetitive	Uncompetitive
10	10	10%	20.0%	13.3%	66.7%
10	10	30%	36.7%	16.6%	46.7%
100	5	30%	26.7%	23.3%	50%
100	10	30%	43.3%	20%	36.7%

per AIC, where r^2 was 0.818 for competitive, noncompetitive and uncompetitive fits. In general, all the competitive, noncompetitive, and uncompetitive fits were very similar from conventional inhibition data, as reflected in the two occasions in Fig. 1. It should be noted that r^2 values are reported here, since r^2 values are frequently inspected as a measure of absolute quality of fit, even though AIC was used to identify the best fitting model.

In Table I, reducing error from 30% to 10% did not improve the ability to identify the competitive model as the correct model (compare 20.0% for%CV = 10% to 36.7% for %CV = 30%). Furthermore, in Table I, when $K\tilde{i}$ was 100 μM and maximum $I/K\tilde{i}$ was 5 (i.e. inhibitor concentration ranged from 0 to 500 μM), the competitive model was the best fitting model only 26.7% of the time. Increasing the maximum $I/K\tilde{i}$ to 10 resulted in the competitive model to be correctly identified 43.3% of the time, which is still poor. This increase in maximum inhibitor concentration from 500 μM to 1,000 μM enhanced the percent substrate inhibition from 76.9% to 86.9%, which may have contributed to the greater reliability to identify the correct model. Unfortunately, such high inhibitor concentration may not be feasible in all cases because of limited inhibitor solubility. Also, changing the weighting from 1 (i.e. no weighting) to weighting of $1/\text{observed}^2$ practically did not change the ability to identify the right model. Using weighting of $1/\text{observed}^2$, the competitive, noncompetitive and uncompetitive models were the best fitting models 30.0%, 23.3%, and 46.7% of the time, respectively, compared to 36.7%, 16.6%, and 46.7% with weighting of 1 (Table I line 2). Similarly, using a different optimization algorithm and different initial conditions had no practical impact. Using the Nelder-Mead simplex algorithm (rather than Gauss-Newton algorithm with Levenberg and Hartley modification), the competitive, noncompetitive and uncompetitive models were the best fitting models 16.7%, 33.3%, and 50.0% of the time. Using initial conditions that differed from the original initial condition by being lower or higher than the estimated values, distribution was 40.0%, 40.0%, and 20.0%.

Notably, the accuracy of the competitive $K\tilde{i}$ estimate was dependent upon%CV, as expected, as well as upon $K\tilde{i}$. The percent of occasions that $K\tilde{i}$ was accurate (i.e. within 20% of true competitive $K\tilde{i}$) was 100%, 36.7%, 63.3%, and 66.7% for the four scenarios listed (top to bottom) in Table I, respectively. Hence, in Table I from conventional inhibition data, very infrequently was the correct model identified and $K\tilde{i}$ accurately estimated.

Simulated Noncompetitive Model Data

Noncompetitive data were simulated for $K\tilde{i} = 100$ μM. Results are summarized in Table II. When maximum ratio of $I/K\tilde{i}$ was 5, the noncompetitive model was correctly identified as the best fitting model only 26.7% of the time. When maximum ratio of $I/K\tilde{i}$ was increased to 10 (i.e. inhibitor concentration up to 1,000 μM), noncompetitive model was correctly identified only 30% of the time. In Table II, $K\tilde{i}$ estimates for the noncompetitive model were accurate 50.0% and 56.7% of the time when inhibitor

Table II Results from Conventional Inhibition Data. Data were Simulated from Noncompetitive Inhibition Model, where Ki, Maximum I/Ki, and Random Error were Varied. Under Best Fitting Model, Values are the Percentage of Times that the Best Fitting Model was Competitive, Noncompetitive, or Uncompetitive. Percentages are Derived from Simulations of 30 Occasions ($n=3$ Per Occasion). AIC was Used to Identify the Best Fitting Model

Ki (μM)	Maximum I/Ki	%CV error	Best fitting model		
			Competitive	Noncompetitive	Uncompetitive
100	5	30%	40.0%	26.7%	33.3%
100	10	30%	30%	30%	40%

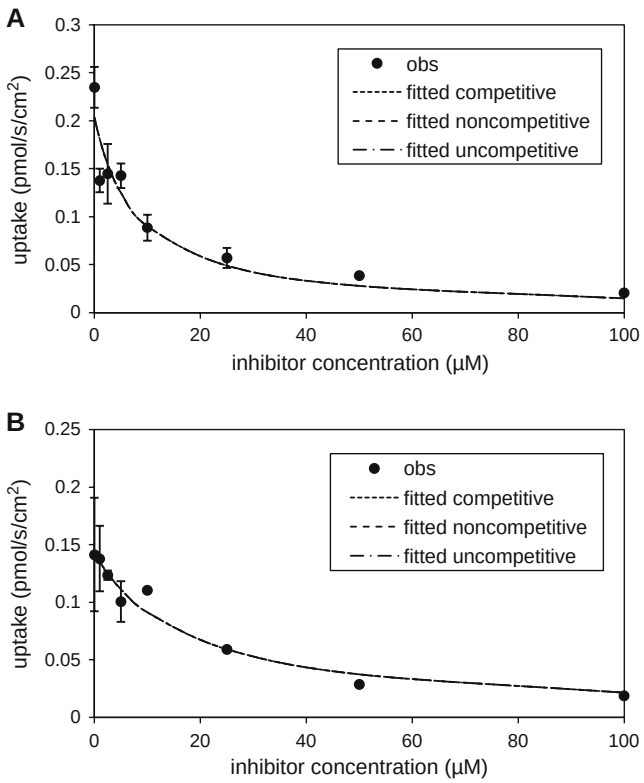

Fig. 1 Fit of all three inhibition models to conventional inhibition data. Data were simulated from competitive inhibition model, where Ki = 10 μM and error was 30%. In panel **A**, the uncompetitive model was the best fitting model, although all three r^2 were about 0.90. In panel **B**, the competitive model was the best fitting model, although all three r^2 were about 0.82. Panels **A** and **B** each present one simulation occasion of the 30 total independent occasions that were conducted. For each occasion, $n = 3$ profiles were simulated. AIC was used to identify the best fitting model.

concentrations were up to 500 μM and 1,000 μM, respectively. These poor results from noncompetitive data (Table II) are practically the same as the poor results from competitive data (Table I), indicating conventional inhibition data is a poor basis to determine type of inhibition.

Analysis of Dixon-Type Data

The second objective was to compare the abilities of the competitive and noncompetitive inhibition models to best fit simulated data where substrate concentration and inhibitor concentration were varied. Varying both substrate concentration and inhibitor concentration is required for traditional Dixon plots, such that these data here are referred to as Dixon-type data. Because substrate concentration is also varied, Dixon-type data are several-fold larger in scope than traditional inhibition data (i.e. objective one above).

Two simulation scenarios were studied that differed in the extent of inhibition. In one scenario, $I/K\tilde{i}$ ranged from 0 to 5, which represents a wide range in inhibitor concentration, compared to typical literature reports. In the second scenario, $I/K\tilde{i}$ ranged from 0 to 1.7, which is a more narrow range, but one that better reflects common practice.

First Simulation Scenario

Simulations covered a range of $I/K\tilde{i}$ from 0 to 5, which reflects a high level of inhibition (i.e. large inhibition concentration, relative to $K\tilde{i}$ potency). In Table III, results indicate that, when competitive inhibition data were simulated with 30% error, the competitive model was the best fitting model 76.7% of the time ($K\tilde{i} = 1$ μM). Otherwise, the noncompetitive model was the best fitting model (23.3% of the time). The uncompetitive model was never the best fitting model.

Fig. 2 shows the simultaneous inhibition profile fits for each of the three substrate concentrations (i.e. 1, 5, and 10 μM). Panels A and B show results from two of the 30 occasions. In panel A, the competitive model was the best fitting model; meanwhile, the noncompetitive model was the best fitting model in panel B. Although the competitive model was usually (and correctly so) the best fitting model (76.7% of the time), Fig. 2 highlights that the quality of fits across all three inhibition models was very similar.

In Table III, when noncompetitive inhibition data were simulated and $K\tilde{i} = 1$ μM, similar fits resulted, in that the correct model (i.e. noncompetitive model) was selected 66.7% of the time. In Table III, results were similarly

Table III Results from Dixon-Type Data. Data were Simulated from Either Competitive or Noncompetitive Inhibition Model, Where Maximum I/Ki = 5 but Ki Varied. Under Best Fitting Model, Values are the Percentage of Times that the Best Fitting Model was Competitive, Noncompetitive, or Uncompetitive. Percentages are Derived from Simulations of 30 Occasions ($n = 3$ Per Occasion). AIC was Used to Identify the Best Fitting Model. Simulated Data Used 30% Error

Ki (μM)	Data origin	Best fitting model		
		Competitive	Noncompetitive	Uncompetitive
1	Competitive	76.7%	23.3%	0%
1	Noncompetitive	30.0%	66.7%	3.33%
100	Noncompetitive	16.7%	76.7%	6.67%

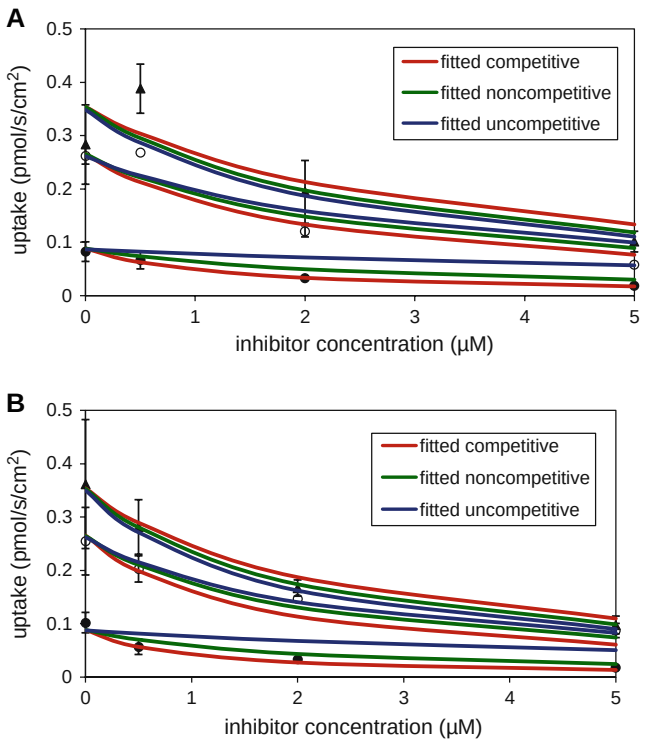

Fig. 2 Simultaneous fits of the competitive inhibition model to Dixon-type data. Data were simulated from competitive inhibition model, where I/Ki ranged from 0–5 and error was 30%. In panel **A**, the competitive model was the best fitting model, although all three r^2 were about 0.68. In panel **B**, the noncompetitive model was the best fitting model, although all three r^2 were about 0.73. Panels **A** and **B** each present one simulation occasion of the 30 total independent occasions that were conducted. For each occasion, $n = 3$ profiles were simulated for each of the three levels of substrate 1 μM (*closed circle*), 2.5 μM (*open circle*), and 5 μM (*closed triangle*). AIC was used to identify the best fitting model.

successful from simulated noncompetitive inhibition data where $K\tilde{i}$=100 μM (76.7% correct). Similarity in results for $K\tilde{i}$=100 μM and Ki=1 μM are due to inhibitor concentration being proportionally changed (i.e. $I/K\tilde{i}$ had the same 0 to 5 range). The extent of inhibition was the same whether $K\tilde{i}$=1 μM or $K\tilde{i}$=100 μM, such that these scenarios in Table III yield similar results. $K\tilde{i}$ estimates were accurate about 50–60% of the time, regardless whether the correct model was the best fitting model.

Second Simulation Scenario: Nonlinear Regression

Simulated experiments covered a range of $I/K\tilde{i}$ from 0 to 1.7, which reflects lower level of inhibition than the first simulation scenario. This more narrow range reflects the common ranges in the literature (10–15). Results for $I/K\tilde{i}$ from 0 to 1.7 in Table IV broadly mimicked results for $I/K\tilde{i}$ from 0 to 5 in Table III. Interestingly, when competitive inhibition data were simulated and 30% error added, the competitive model was the best fitting model 76.7% of the time, the noncompetitive model was best fitting 23.3% of the time, and the uncompetitive model was never the best fitting model. These results for $I/K\tilde{i}$ from 0 to 1.7 (Table IV) are identical to those results for $I/K\tilde{i}$ from 0 to 5 (Table III). Comparing Table III and IV for simulated noncompetitive inhibition data show the noncompetitive model was selected about 60–80% of the time. Table IV also shows results when competitive data simulated with 20% error. There was no appreciable difference in results between 20% and 30% error (i.e. 80% correct *versus* 76.7% correct).

Above results indicate that nonlinear regression was modestly successful in identifying the type of inhibition (range from 60.0% to 80.0% in Tables III and IV). Hence, we suggest caution in concluding inhibition type, even when employing comprehensive data where both substrate and inhibitor concentration are varied. Perhaps not surprising, level of success from this more compressive data was greater than from conventional inhibition data, where the success rate (20.0–43.3%) was poor.

Even in spite of this moderate success rate from Dixon-type data, nonlinear regression frequently did not estimate $K\tilde{i}$ accurately. For the simulated competitive and noncompetitive data with $K\tilde{i}$=1 μM with added 30% error (Table III), an accurate estimate of $K\tilde{i}$ was obtained only 56.7% and 50.0% of the time, respectively. For the simulated noncompetitive data with $K\tilde{i}$=100 μM, an accurate estimate of $K\tilde{i}$ was obtained only 63.3% of the time.

Table IV Results from Dixon-type Data. Data were Simulated from Either Competitive or Noncompetitive Inhibition Model, Where Maximum I/Ki = 1.7 and Ki = 58. Under Best Fitting Model, Values are the Percentage of Times that the Best Fitting Model was Competitive, Noncompetitive, or Uncompetitive. Percentages are Derived from Simulations of 30 Occasions ($n = 3$ Per Occasion). AIC was Used to Identify the Best Fitting Model

Ki (μM)	%CV error	Data origin	Best fitting model		
			Competitive	Noncompetitive	Uncompetitive
58	20%	Competitive	80.0%	20.0%	0%
58	30%	Competitive	76.7%	23.3%	0%
58	30%	Noncompetitive	20.0%	60.0%	20.0%

Second Simulation Scenario: Dixon Plot Analysis

While nonlinear regression is the primary focus, secondary analysis is present here, where Dixon-type data is subjected to Dixon plot analysis. Linearized forms of inhibition models such as Dixon plots and Lineweaver-Burk plots are commonly used to elucidate type of inhibition and inhibition constant $K\tilde{i}$. The Dixon plot has been reported to have some limitations, and many authors have suggested use of nonlinear regression rather than the linearized form to calculate $K\tilde{i}$ (16,17). Yet, the Dixon plot is still frequently used to evaluate the mode of inhibition (18–20). Surprisingly, the accuracy of the Dixon plot to correctly identify the type of inhibition has never been assessed.

Fig. 3 shows Dixon plots from simulated noncompetitive data. In a Dixon plot, noncompetitive inhibition provides profiles that intersect on the *x*-axis. In panel A of Fig. 3, inhibition appears to be competitive (i.e. incorrect conclusion), since the profiles intersect above the *x*-axis. In panel B, two profiles intersect above the *x*-axis, while two others intersect on the *x*-axis, such that the correct inhibition type (i.e. noncompetitive inhibition) was not easily concluded. In both panels A and B, this classic approach to assess for noncompetitive inhibition failed to conclude noncompetitive inhibition. From this graphical/visual approach to discriminate competitive *versus* noncompetitive *versus* uncompetitive inhibition, the noncompetitive model performed poorly. For simulated noncompetitive data with 30% error, the correct model was concluded only on two of 30 occasions. On 22 of the 30 occasions, it was not readily possible to identify the type of inhibition (i.e. appear like Fig. 3 panel B). For simulated competitive data with either 20% or 30% added error, the correct model was identified only on four of the 30 occasions.

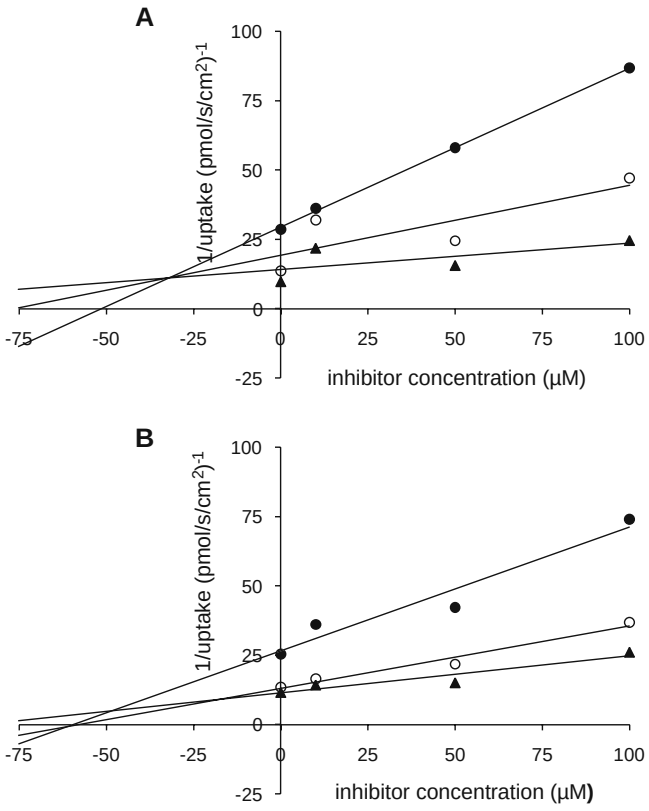

Fig. 3 Dixon plots of Dixon-type data. Data were simulated from noncompetitive inhibition model, where I/Ki ranged from 0–1.7. Each panel **A** and **B** are data from separate occasions of the 30 total independent occasions that were simulated. In spite of this sameness in data origin, panel **A** is visually different from panel **B**. In panel **A**, inhibition appears to be competitive, since the three lines intersect above the *x*-axis. In panel **B**, inhibition appears to be indeterminate, since two lines intersect above the *x*-axis, while another pair intersects on the *x*-axis. In each panel, substrate concentration is 1 μM (*closed circle*), 2.5 μM (open circle), and 5 μM (*closed triangle*). Simulated data used 30% error. For each occasion, $n = 3$ profiles were simulated for each of the three levels of substrate.

Second Simulation Scenario: Summary

Overall results indicate that nonlinear regression was moderately successful in identifying the type of inhibition (about 60–80% of the time). This level of reliability was observed for both the competitive and noncompetitive inhibition model, as well as for both 20% and 30% error. However, nonlinear regression often did not estimate $K\tilde{i}$ accurately (i.e. within 20% of true $K\tilde{i}$). For the simulated competitive data with added 30% error, an accurate estimate of $K\tilde{i}$ was obtained only 30% of the time. When added error was reduced from 30% to 20%, performance improved, where $K\tilde{i}$ estimates were accurate 56.7% of the time. Meanwhile, for the noncompetitive data with added 30% error, accurate $K\tilde{i}$ was estimated only 50% of the time.

Analysis of Nonconventional Inhibition Data

From objective one, conventional inhibition data performed poorly in identifying the correct model. This finding from this most common type of inhibition data (i.e. uptake from a single, fixed substrate concentration as a function of a range of inhibitor concentrations) motivated an analysis to assess whether similar inhibition data, but varying substrate concentration and not inhibitor concentration, could improve performance.

Simulated Competitive Model Data

Table V summarizes results obtained from simulated competitive data where substrate concentration was varied and inhibitor concentration was fixed at a single level. Simulations involved 30% error and covered a range of scenarios, where $K\tilde{i}$ was 5 μM or 500 μM, and the ratio of $I/K\tilde{i}$ was 0.01, 1 or 100. All figures relating to the third

Table V Results from Nonconventional Inhibition Data. Data were Simulated from Competitive Inhibition Model, Where Kt and I/Ki were Varied. Under Best Fitting Model, Values are the Percentage of Times that the Best Fitting Model was Competitive, Noncompetitive, or Uncompetitive Percentages are Derived from Simulations of 30 Occasions ($n=3$ Per Occasion). AIC was Used to Identify the Best Fitting Model. Simulated Data Used 30% Error

Kt (μM)	I/Ki	Best fitting model		
		Competitive	Noncompetitive	Uncompetitive
5	0.01	50.0%	16.7%	33.3%
5	1	100%	0%	0%
5	100	100%	0%	0%
500	0.01	50.0%	10.0%	40.0%
500	1	100%	0%	0%
500	100	100%	0%	0%

objective are in terms of substrate uptake *versus* substrate concentration; such inhibition plots are uncommon, since inhibitor concentration is fixed at a single level and not varied, while substrate concentration is varied. Fig. 4 differs from Fig. 1, which reflects conventional inhibition data.

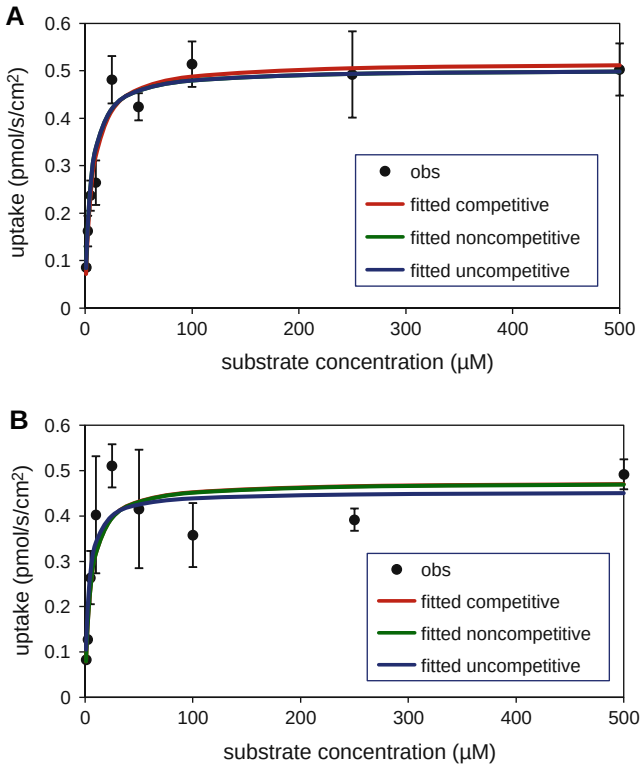

Fig. 4 Fit of all three inhibition models to nonconventional inhibition data. Data were simulated from competitive inhibition model, where I/Ki = 0.01 and error was 30%. In panel **A**, the competitive model (*red*) was the best fitting model, although all three r^2 were about 0.73. The noncompetitive fit (*green*) overlaps with the uncompetitive fit (*blue*). In panel **B**, the uncompetitive model was the best fitting model, although all three r^2 were about 0.89. The competitive fit overlaps with the noncompetitive fit. Panels **A** and **B** each present one simulation occasion of the 30 total independent occasions that were conducted. For each occasion, $n=3$ profiles were simulated. AIC was used to identify the best fitting model.

In Table V, when $I/K\tilde{i}$ was 0.01, the competitive model was the best fitting model only 50% of the time for $K\tilde{i}$= 5 μM or 500 μM. Fig. 4 shows all three model fits to simulated competitive data on two separate occasions when $K\tilde{i}$=5 μM. In Fig. 4 Panel A, the competitive model was the best fitting model, where r^2=0.894, 0.892 and 0.892 for competitive, noncompetitive and uncompetitive fits, respectively. In panel B, the uncompetitive model was the best fitting model, where r^2=0.728, 0.728, and 0.740 for competitive, noncompetitive and uncompetitive fits, respectively. In general, the noncompetitive fit was very similar to the competitive fit, such that noncompetitive was infrequently the best fitting model (i.e. less than 20% of time). Meanwhile, uncompetitive fits were similar to, but sufficiently different from, the other two models, such that it was best fitting about one-third of the time.

In Table V, the competitive model performed better when $I/K\tilde{i}$ was increased from 0.01 to 1 and 100, where the competitive model was always the best fitting model. Fig. 5 shows all three fits to data simulated from the

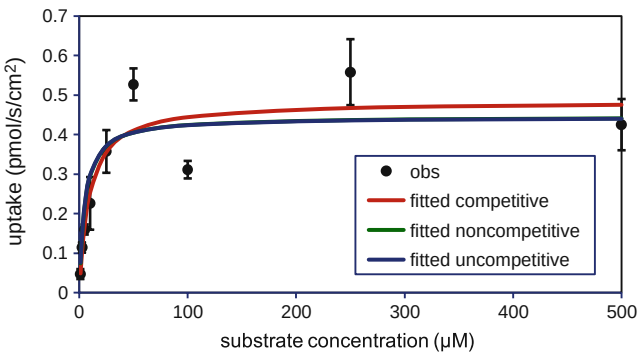

Fig. 5 Fit of all three inhibition models to nonconventional inhibition data. Data were simulated from competitive inhibition model, where I/Ki = 1 and error was 30%. The competitive model was always the best fitting model, although all three r^2 were about 0.84. The noncompetitive and uncompetitive fits overlap. The plot presents one simulation occasion of the 30 total independent occasions that were conducted. For each occasion, $n=3$ profiles were simulated. AIC was used to identify the best fitting model.

competitive inhibition model when ratio was 1. In Table V, $K\tilde{i}$ did not have a notable impact. Results were similar whether $K\tilde{i}$=5 μM or 500 μM.

Simulated Noncompetitive Model Data

Noncompetitive inhibition data were simulated with $K\tilde{i}$= 5 μM. Results are summarized in Table VI and demonstrate the noncompetitive model is less frequently the best fitting model, compared to the competitive model (Table V). However, as above, the correct model was always the best fitting model when $I/K\tilde{i}$ was large (i.e. $I/K\tilde{i}\geq 10$). Interestingly, when $I/K\tilde{i}\leq 1$, the noncompetitive model was infrequently the best model (3.33%). Unlike the simulated competitive data, $I/K\tilde{i}$ needed to be 10 (rather than 1) for the noncompetitive model to be the best fitting model 100% of the time. While the competitive model was always the best fitting model when $I/K\tilde{i}=1$, the noncompetitive model was infrequently the best fitting model when $I/K\tilde{i}=1$.

Overall Performance of Nonconventional Inhibition Data

For the third objective, overall results show that the use of nonconventional data had modest success in identifying the correct model. The level of success depended upon the ratio of $I/K\tilde{i}$, where greater inhibition promoted higher reliability. When the competitive model was the correct model, success was 100% when $I/K\tilde{i}$ was 1 or larger. When the noncompetitive model was the correct model, success was 100% when $I/K\tilde{i}$ was 10 or larger. These results are a marked contrast to findings using conventional data, where success was 30–35%. Overall findings here suggest nonconventional data merits further examination as an approach to employ minimal data and determine inhibition type. Interestingly, nonconventional data was only a fraction in scope of the Dixon-type data, but performed better than analysis that used Dixon-type data.

A possible explanation of the better performance of the nonconventional data is the greater inhibition afforded by the nonconventional data. For example, for nonconventional data, the best fitting model being the correct model depended upon $I/K\tilde{i}$, where greater inhibition promoted higher reliability. For higher $I/K\tilde{i}$, nonlinear regression with AIC frequently performed well, in terms of the correct model being the best fitting model, even when the absolute difference in AIC values and r^2 values between competing models were small. When data were simulated using a competitive inhibition model, nonlinear regression with AIC usually was able to identify the competitive inhibition model with moderate success (about 75% of the time). This level of success was about the same when data were noncompetitive, although noncompetitive data were more sensitive to the $I/K\tilde{i}$ ratio. For example, when $I/K\tilde{i}=1$ and 30% error, the extent of inhibition reached 45%, allowing the competitive inhibition model to be correctly identified all the time.

While the ability to reliably characterize competitive inhibition as competitive required only 45% inhibition, it should be recognized that low inhibitor solubility can limit achieving even this necessary level of inhibition (21). Compared to competitive inhibition with 30% error (Table V), less desirable results were observed for the noncompetitive inhibition model with 30% error (Table VI). When $I/K\tilde{i}$ was even as high as 1 (i.e. 50% inhibition), the noncompetitive inhibition model was identified only 3.3% of the time; usually, the competitive inhibition model was incorrectly identified as the model. When $I/K\tilde{i}=10$, the extent of inhibition reached 90%, allowing the noncompetitive inhibition model to be correctly identified all the time. For both the competitive and noncompetitive models, a specific level of inhibition was required to reliably identify the correct model. For the competitive model, 45% inhibition was sufficient. For noncompetitive model, 50% inhibition was insufficient, but rather required 90% inhibition, which is a two-fold greater requirement. This high level of inhibition may be problematic if a compound suffers from modest inhibition potency and/or low solubility.

Table VI Results from Nonconventional Inhibition Data. Data were Simulated from Noncompetitive Inhibition Model, Where I/Ki were Varied and Kt = 5 μM. Under Best Fitting Model, Values are the Percentage of Times that the Best Fitting Model was Competitive, Noncompetitive, or Uncompetitive Percentages are Derived from Simulations of 30 Pccasions (n = 3 Per Occasion). AIC was Used to Identify the Best Fitting Model. Simulated Data Used 30% Error

Kt (μM)	Ratio (I/Ki)	Best fitting model		
		Competitive	Noncompetitive	Uncompetitive
5	0.01	60.0%	3.33%	36.7%
5	1	53.3%	3.33%	43.3%
5	10	0%	100%	0%
5	100	0%	100%	0%

Reflections from Experimental Data

Ursodeoxycholic acid is expected to bind to ASBT at the same binding site as taurocholic acid, since they are both native bile acids and share high chemical similarity. Moreover, ASBT is a relatively small transporter, with a molecular weight of 43 kDa (22). The taurine conjugate of ursodeoxycholate has been identified as a competitive inhibitor of taurocholate (23).

Conventional Inhibition Data

Inhibition studies were performed over a range of ursodeoxycholate concentrations, while substrate (taurocholate) concentration was maintained at 2.5 μM. The maximum ratio of $I/K\tilde{i}$ was 7.1, which was in the range of the simulations performed. Competitive $K\tilde{i}$ for ursodeoxycholate was found to be 35.2 ± 2.67 μM, which is similar to the previous report (24). Fig. 6 panel A shows model fits to the conventional inhibition data. As expected from simulations, the competitive, noncompetitive and uncompetitive fits in Fig. 6 panel A were very similar to each other. The noncompetitive model was the best fitting model, which we believe is an incorrect model. For simulations that were similar to this experimental condition (Table I where $I/K\tilde{i}=10$ and%CV = 10%), the competitive and noncompetitive models were best fitting 20.0% and 13.3% of the time.

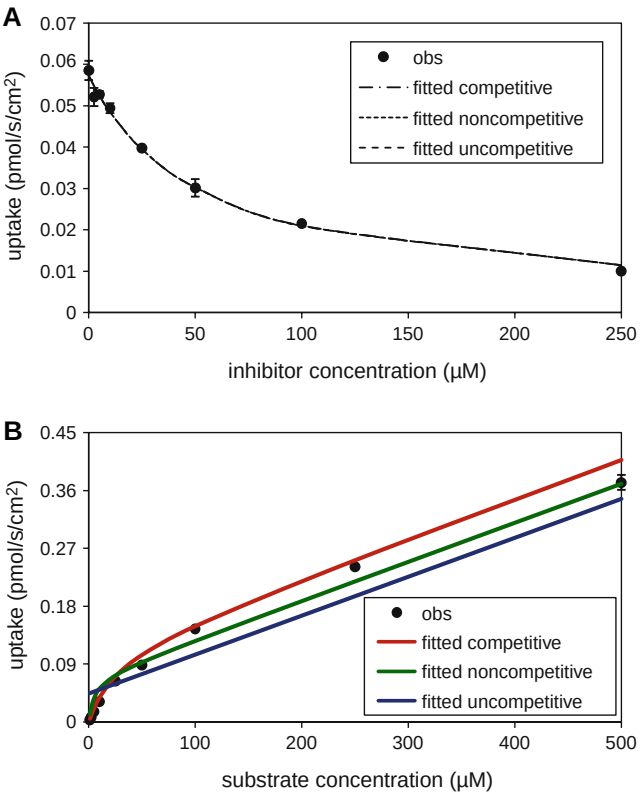

Fig. 6 Results from experimental data. Panel **A** shows model fits to conventional inhibition data, where substrate concentration is 2.5 μM. The noncompetitive model was the best fitting model, although all three r^2 were about 0.99. Panel **B** shows fits to nonconventional inhibition data, when I/Ki = 5. The competitive model was the best fitting model, although r^2 was about 0.99 for competitive and noncompetitive fit and 0.98 for uncompetitive fit. Each point is mean ± SEM of three measurements.

Nonconventional Inhibition Data

Nonconventional inhibition data was obtained under two sets of conditions, where $I/K\tilde{i}$ was designed to vary, employing an expected $K\tilde{i}$ value of 35.2 μM from the conventional inhibition results above. In both conditions, taurocholate concentration ranged from 0 to 500 μM, but where $I/K\tilde{i}=1$ in one set (i.e. $I=35.2$ μM), while $I/K\tilde{i}=5$ in the second set (i.e. $I=176$ μM).

When $I/K\tilde{i}=1$, the noncompetitive model (incorrect model) was the best fitting model. When $I/K\tilde{i}=5$, the competitive model (correct model) was the best fitting model; Fig. 6 panel B plots the result. Experimental results are partially consistent with simulation results (Table V). Simulation results in Table V suggest very high accuracy to identify the competitive model as the correct model when $I/K\tilde{i}=1$ or higher (e.g. high accuracy when the percentage of inhibition reached 45.4% or greater). Here, the presumably correct model (i.e. competitive model) was concluded only when $I/K\tilde{i}=5$, where the percentage of inhibition reaches 80.6%. Overall, with the assumption that ursodeoxycholate competitively inhibits taurocholate, nonconventional inhibition data appears to have performed better than conventional inhibition data. However, these experimental results suggest that even simulation results, which anticipate modest ability for nonlinear regression to identify the correct model, may be too optimistic.

Dixon-Type Data

Dixon-type data was generated by varying both inhibitor and substrate concentrations. Ursodeoxycholate concentrations were 0, 25, 50, and 100 μM (i.e. four levels). Taurocholate concentrations were 1, 2.5, and 5 μM (i.e. three levels). In pooling uptake data from all 12 experimental conditions, simultaneous nonlinear regression was applied to this Dixon-type data. Figure S1 panel A (Supplemental Material) shows the competitive, noncompetitive and uncompetitive fits. The competitive model was the best fitting model. Figure S1 panel B (Supplemental Material) shows the traditional Dixon plot for this data set. All three profiles did not intersect at one point, as required for competitive inhibition. Two points of intersection were above the *x*-axis. Thus, the traditional Dixon plot appears to conclude

competitive inhibition. It was not possible to measure $K\tilde{i}$ from the plot, since all the profiles did not intersect at one point.

Comparison Between Conventional and Nonconventional Inhibition Data

Findings here are notable in that nonconventional inhibition data appears more promising than conventional inhibition data in trying to identify the correct inhibition model from *in vitro* assessment. Hence, error-free simulations were performed. For conventional inhibition data, when there is no error added to uptake values and $I/K\tilde{i}=100$, 98.5% inhibition occurs for competitive model, while 99% inhibition occurs for noncompetitive model. However, the visual difference in simulated uptake between models is very small (Fig. 7). This visual similarity, even under error-free conditions, explains the difficulty in correctly identifying the correct model from conventional inhibition data under this common situation.

Meanwhile, for nonconventional inhibition data, simulated uptake from competitive and noncompetive models are more readily discernable from another. Fig. 8 illustrates error-free uptake over a range of $I/K\tilde{i}$ scenarios from competitive, noncompetitive, and uncompetitive inhibitions. The difference between competitive and noncompetitive models is evident at even the low $I/K\tilde{i}$ ratio of 1. The difference between noncompetitive and uncompetitive models requires the higher $I/K\tilde{i}$ ratio of 10 (i.e. greater inhibition to discern these model differences). These error-free simulations support observations above from simulation and experimental findings that nonconventional inhibition data appears to be the better approach to collect data in order to elucidate type of inhibition. Further evaluation is merited.

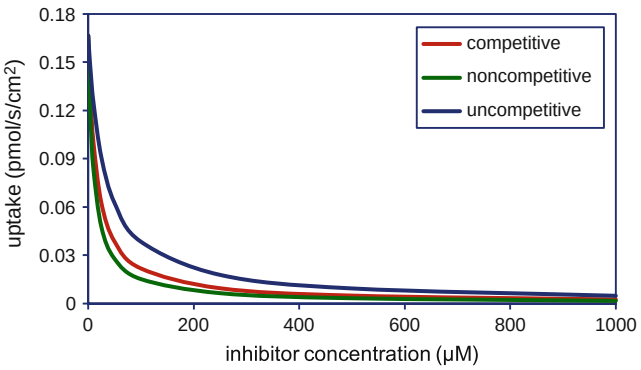

Fig. 7 Inhibition profiles from error-free conventional inhibition data, when Ki = 10 μM and maximum I/Ki = 100 and S = 2.5 μM. All the inhibition models were visually very similar to each other.

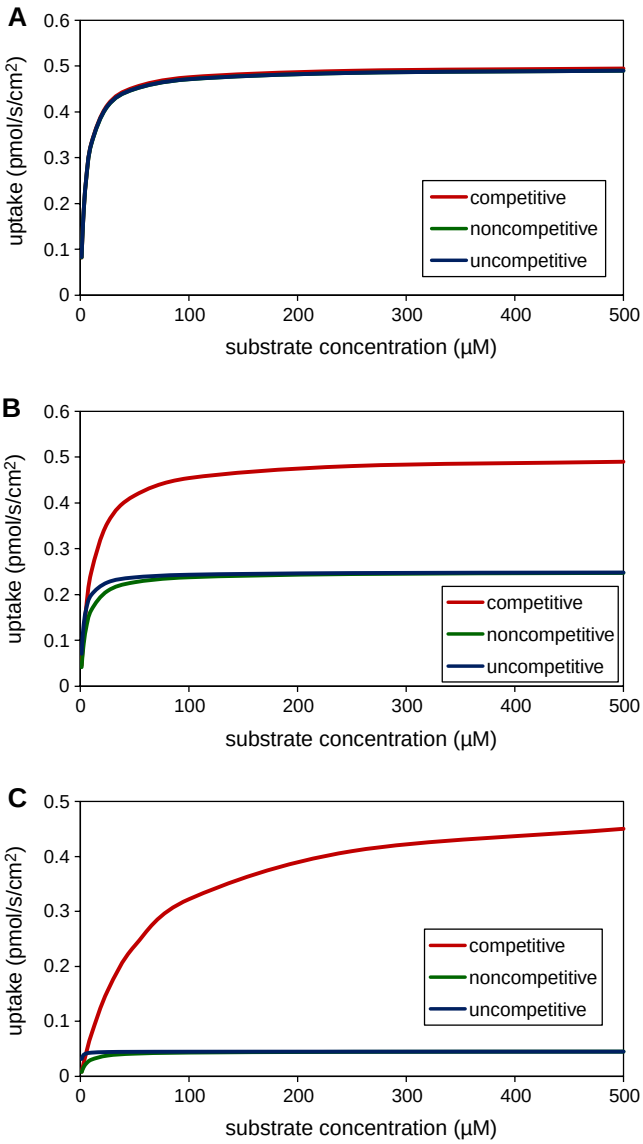

Fig. 8 Inhibition profiles from error-free nonconventional inhibition data. Panel **A** shows the three profiles are essentially identical where I/Ki = 0.01. Panel **B** employs I/Ki = 1 and shows the competitive model to be visually different from the noncompetitive and uncompetitive models at this higher I/Ki ratio. However, the noncompetitive and uncompetitive models were similar to one another. Panel **C** employs I/Ki = 10 and shows the competitive model is easily discernable from the other two models. The noncompetitive and uncompetitive models also differed from one another between 0 μM and 50 μM (Figure S2 in supplemental data).

CONCLUSIONS

Analysis here examined the conditions and extent to which nonlinear regression results can be relied upon. For conventional inhibition data, nonlinear regression with AIC performed poorly for both the competitive and noncompetitive inhibition models. For Dixon-type data, nonlinear regression yielded moderately better results. Interestingly, nonconventional inhibition data performed well, with higher ratio of $I/$

Ki providing better results. Nonconventional inhibition data merits further consideration.

ACKNOWLEGEMENTS

This work was supported in part by National Institutes of Health (grant DK67530). WinNonlin software was kindly donated by Pharsight Corp. (Mountain View, CA).

REFERENCES

1. Rais R, Acharya C, Tririya G, Mackerell AD, Polli JE. Molecular switch controlling the binding of anionic bile acid conjugates to human apical sodium-dependent bile acid transporter. J Med Chem. 2010;53:4749–60.
2. Gonzalez PM, Acharya C, Mackerell Jr AD, Polli JE. Inhibition requirements of the human apical sodium-dependent bile acid transporter (hASBT) using aminopiperidine conjugates of glutamyl-bile acids. Pharm Res. 2009;26:1665–78.
3. Zheng X, Ekins S, Raufman JP, Polli JE. Computational models for drug inhibition of the human apical sodium-dependent bile acid transporter. Mol Pharm. 2009;6:1591.
4. Diao L, Ekins S, Polli JE. Novel inhibitors of human organic cation/carnitine transporter (hOCTN2) via computational modeling and *in vitro* testing. Pharm Res. 2009;26:1890–900.
5. Lin CJ, Akarawut W, Smith DE. Competitive inhibition of glycylsarcosine transport by enalapril in rabbit renal brush border membrane vesicles: interaction of ACE inhibitors with high-affinity H+/peptide symporter. Pharm Res. 1999;16:609–15.
6. Akarawut W, Lin CJ, Smith DE. Noncompetitive inhibition of glycylsarcosine transport by quinapril in rabbit renal brush border membrane vesicles: effect on high-affinity peptide transporter. J Pharmacol Exp Ther. 1998;287:684–90.
7. Lau AJ, Chang TK. Inhibition of human CYP2B6-catalyzed bupropion hydroxylation by Ginkgo biloba extract: effect of terpene trilactones and flavonols. Drug Metab Dispos. 2009;37:1931–7.
8. Frank H and Althoen S, C. Statistics: concepts and applications. 1994; 853.
9. Akaike A. Posterior probabilities for choosing a regression model. Annals of the Institute of Mathematical Statistics. 1978;30A9–14.
10. Bhattacharyya A, Mazumdar Leighton S, Babu CR. Bioinsecticidal activity of Archidendron ellipticum trypsin inhibitor on growth and serine digestive enzymes during larval development of Spodoptera litura. Comp Biochem Physiol C Toxicol Pharmacol. 2007;145:669–77.
11. Ismair MG, Kullak-Ublick GA, Blakely RD, Fried M, Vavricka SR. Tegaserod inhibits the serotonin transporter SERT. Digestion. 2007;75:90–5.
12. Je JY, Kim SK. Water-soluble chitosan derivatives as a BACE1 inhibitor. Bioorg Med Chem. 2005;13:6551–5.
13. Martin-Venegas R, Rodriguez-Lagunas MJ, Geraert PA, Ferrer R. Monocarboxylate transporter 1 mediates DL-2-Hydroxy-(4-methylthio)butanoic acid transport across the apical membrane of Caco-2 cell monolayers. J Nutr. 2007;137:49–54.
14. Narawa T, Tsuda Y, Itoh T. Chiral recognition of amethopterin enantiomers by the reduced folate carrier in Caco-2 cells. Drug Metab Pharmacokinet. 2007;22:33–40.
15. Wong IL, Chan KF, Tsang KH, Lam CY, Zhao Y, Chan TH, *et al.* Modulation of multidrug resistance protein 1 (MRP1/ABCC1)-mediated multidrug resistance by bivalent apigenin homodimers and their derivatives. J Med Chem. 2009;52:5311–22.
16. Kakkar T, Boxenbaum H, Mayersohn M. Estimation of Ki in a competitive enzyme-inhibition model: comparisons among three methods of data analysis. Drug Metab Dispos. 1999;27:756–62.
17. Schlamowitz M, Shaw A, Jackson WT. Limitations of the Dixon plot for ascertaining naure of enzyme inhibition. Tex Rep Biol Med. 1969;27:483–8.
18. Duan P, You G. Novobiocin is a potent inhibitor for human organic anion transporters. Drug Metab Dispos. 2009;37:1203–10.
19. Lan T, Rao A, Haywood J, Davis CB, Han C, Garver E, *et al.* Interaction of macrolide antibiotics with intestinally expressed human and rat organic anion-transporting polypeptides. Drug Metab Dispos. 2009;37:2375–82.
20. Knutter I, Wollesky C, Kottra G, Hahn MG, Fischer W, Zebisch K, *et al.* Transport of angiotensin-converting enzyme inhibitors by H+/peptide transporters revisited. J Pharmacol Exp Ther. 2008;327:432–41.
21. Rais R, Gonzalez PM, Zheng X, Wring SA, Polli JE. Method to screen substrates of apical sodium-dependent bile acid transporter. AAPS J. 2008;10:596–605.
22. Balakrishnan A, Polli JE. Apical sodium dependent bile acid transporter (ASBT, SLC10A2): a potential prodrug target. Mol Pharm. 2006;3:223–30.
23. Craddock AL, Love MW, Daniel RW, Kirby LC, Walters HC, Wong MH, *et al.* Expression and transport properties of the human ileal and renal sodium-dependent bile acid transporter. Am J Physiol. 1998;274:G157–69.
24. Balakrishnan A, Sussman DJ, Polli JE. Development of stably transfected monolayer overexpressing the human apical sodium-dependent bile acid transporter (hASBT). Pharm Res. 2005;22:1269–80.